Hindawi Publishing Corporation
Discrete Dynamics in Nature and Society
Volume 2012, Article ID 283179, 9 pages
doi:10.1155/2012/283179

Research Article

An Algorithm to Automatically Detect the Smale Horseshoes

Qingdu Li,[1,2] Lina Zhang,[2] and Fangyan Yang[2]

[1] *Key Laboratory of Network Control & Intelligent Instrument of Ministry of Education, Chongqing University of Posts and Telecommunications, Chongqing 400065, China*
[2] *Institute for Nonlinear Circuits and Systems, Chongqing University of Posts and Telecommunications, Chongqing 400065, China*

Correspondence should be addressed to Qingdu Li, liqd@cqupt.edu.cn

Received 9 August 2011; Revised 10 November 2011; Accepted 15 December 2011

Academic Editor: Nikos I. Karachalios

Smale horseshoes, curvilinear rectangles and their U-shaped images patterned on Smale's famous example, provide a rigorous way to study chaos in dynamical systems. The paper is devoted to constructing them in two-dimensional diffeomorphisms with the existence of transversal homoclinic saddles. We first propose an algorithm to automatically construct "horizontal" and "vertical" sides of the curvilinear rectangle near to segments of the stable and of the unstable manifolds, respectively, and then apply it to four classical chaotic maps (the Duffing map, the Hénon map, the Ikeda map, and the Lozi map) to verify its effectiveness.

1. Introduction

Among a variety of mathematical characteristics of chaos, the existence of a horseshoe (by S. Smale) has been recognized as the most important signature of chaos from geometrical point of view. The horseshoe theory is based on the geometry of continuous maps on some subsets of interest in state space. Here the images of the subsets can be computed reliably, so rigorous investigation of chaos becomes possible even for systems without explicit solutions.

Although the theory provides a powerful tool for many rigorous studies of chaos, such as estimating topological entropy, verifying existence of chaos, and revealing invariant sets of chaotic attractors, it has not been used extensively like many other numerical methods, such as computing Lyapunov exponents or bifurcation diagrams. Beside of reliable computation based on interval arithmetic, another main reason is probably because it is not as convenient to find horseshoes in practical systems as other nonrigorous methods. In recent years,

much work has been done in providing more applicable criteria to guarantee the existence of horseshoes [1–4]. The criteria have been applied to many dynamical systems [3, 5–7]. Recently, a progress was made in [8] which proposed a method for finding horseshoes in two-dimensional (2D) chaotic maps (or Poincaré maps). The method was implemented with A MATLAB GUI program (http://www.mathworks.com/matlabcentral/fileexchange/14075) to help readers to improve efficiency and has been successfully applied to some novel cases, for example, a hyperchaotic spacecraft circuit [9], the fractional-order unified system [10], and so forth. However, researches still need to find horseshoes manually with their own experiences. So this paper proposes a simple algorithm to automatically detect the Smale horseshoes in 2D chaotic maps.

The paper is organized as follows. Section 2 revisits the Smale horseshoe and tries finding some key points; Section 3 introduces our algorithm as well as some classical examples; Section 4 draws conclusions.

2. The Smale Horseshoe

First let us recall the notion of the Smale horseshoe. Consider a square $S \subset R^2$ with four vertices A, B, C, and D. The diffeomorphism

$$h : S \longrightarrow h(S) \subset R^2 \tag{2.1}$$

is defined as follows: First the map contracts the square S horizontally with a factor less than $1/2$, stretches it vertically with a factor greater than 2, then folds it like a horseshoe, and puts it back on the square S, as shown in Figure 1, where h sends A to A′, B to B′, C to C′, and D to D′.

As shown in Figure 1, p is a period-1 saddle point, W^s and W^u are the corresponding stable manifold $\{z : h^n(z) \to p \text{ as } n \to +\infty\}$ and unstable manifold $\{z : h^n(z) \to p \text{ ass } n \to -\infty\}$ of p. Another intersection q is what Poincaré called a homoclinic point. The homoclinic point here is transverse in the sense that the stable and unstable manifolds are not tangent at q.

The main point in the Smale horseshoe is not the shape of the square S and its image of under h, but the "crossing" relation that $h(S)$ goes through S twice between AD and CB while any point of A′B′ and C′D′ does not locate inside of S, which guarantees the existence of the two disjoint blocks S_0 and S_1. So the Smale horseshoes can be used extensively in many practical systems, where S will no longer be a square.

3. The Algorithm for Finding the Smale Horseshoes in 2D Maps

For convenience, we use a subscript to denote the iteration times, for example, $q_1 = h(q)$, $q_0 = q$, $q_{-1} = h^{-1}(q)$, and use a combination of two points with a different cap to denote a piece of a different manifold between them; for example, $\widehat{pq}$ denotes the piece of W^u from p to q, and $\underbrace{qp}$ denotes the piece of W^s from q to p.

The key to detecting a Smale horseshoe is the boundary of S. For the standard case demonstrated in Figure 1, the process is very easy. When we iterate each point of $\underbrace{qq_1}$ reversely from q to q_1, $\underbrace{q_{-1}q} = h^{-1}(\underbrace{qq_1})$ must intersect $\widehat{pq}$ three times at least. The first and last intersection points are q_{-1} and q, respectively. We denote the second one with r_{-1}. Let S_W be

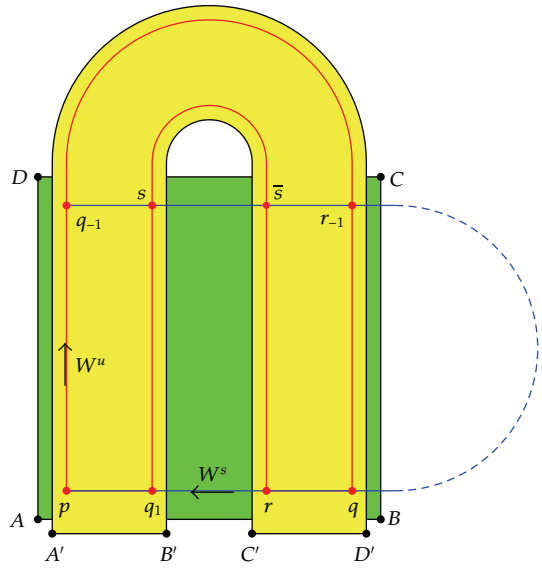

Figure 1: Smale horseshoe.

a block with four sides: $\widehat{pq_{-1}}$, $\overbrace{q_{-1}r_{-1}}$, $\widehat{r_{-1}q}$, and $\overbrace{qp}$. The map h sends the sides to $\widehat{pq}$, $\overbrace{qr}$, $\widehat{rq_1}$, and $\overbrace{q_1p}$, respectively. Here, $\overbrace{q_{-1}r_{-1}}$ and $\widehat{rq_1}$ intersect twice at s and $\bar{s}$, respectively. It is obvious that $h(S_W)$ and S_W also satisfy the relation of the Smale horseshoe.

However, for a practical chaotic map $f : R^2 \to R^2$, we will face the following five difficulties. (1) There are many saddle points with all periods; we have to pick a proper one to ensure the rest computation, but p in Figure 1 is only period-1. (2) Both W^s and W^u have two branches, but Figure 1 only illustrates one of them. (3) The two eigenvalues of f at p can be positive or negative, but Figure 1 only illustrates the positive one. (4) h has a horseshoe, but f may not. (5) S_W cannot be applied in rigorous studies of chaos because there exist unavoidable numerical errors in practical computations. An algorithm which can automatically detect a Smale horseshoe must handle the above difficulties.

So in our algorithm, we first find a transverse homoclinic point, then we locate S_W using the stable and unstable manifolds, and last we extend the boundary of S_W outside to get S. The algorithm is as follows with its detailed flowchart illustrated in Figure 2.

(1) Find a periodic point p at first. Supposing that p has period N, we compute the eigenvalues of the Jacobian matrix of f^N at p. If one eigenvalue locates in the inside of the unit circle and the other one locates outside the unit circle, then p is a saddle point of f^N; otherwise, we need to find another p and try again. If any of the eigenvalues is negative, then we take $I = 2$; otherwise, $I = 1$. Let $g = f^{IN}$; then, we find a transverse homoclinic point q by computing the corresponding stable and unstable manifolds of p.

(2) Detect S_W by finding a proper iteration time M and a proper intersection point r with the following procedure. Let $M = 1$ and $r = p$, that is, $r_{1-M} = p$. Iterate the map g reversely for each point of $\overbrace{q_{1-M}r_{1-M}}$ from q_{1-M} to r_{1-M} until $\overbrace{q_{-M}r_{-M}}$ intersects $\widehat{pq}$ again (not q_{-M}). If the new intersection point is not in $\widehat{r_{1-M}q}$, then set r_{-M} to be r_{1-M}, $M = M + 1$ and try it again; otherwise, set r_{-M} to be the point and compute

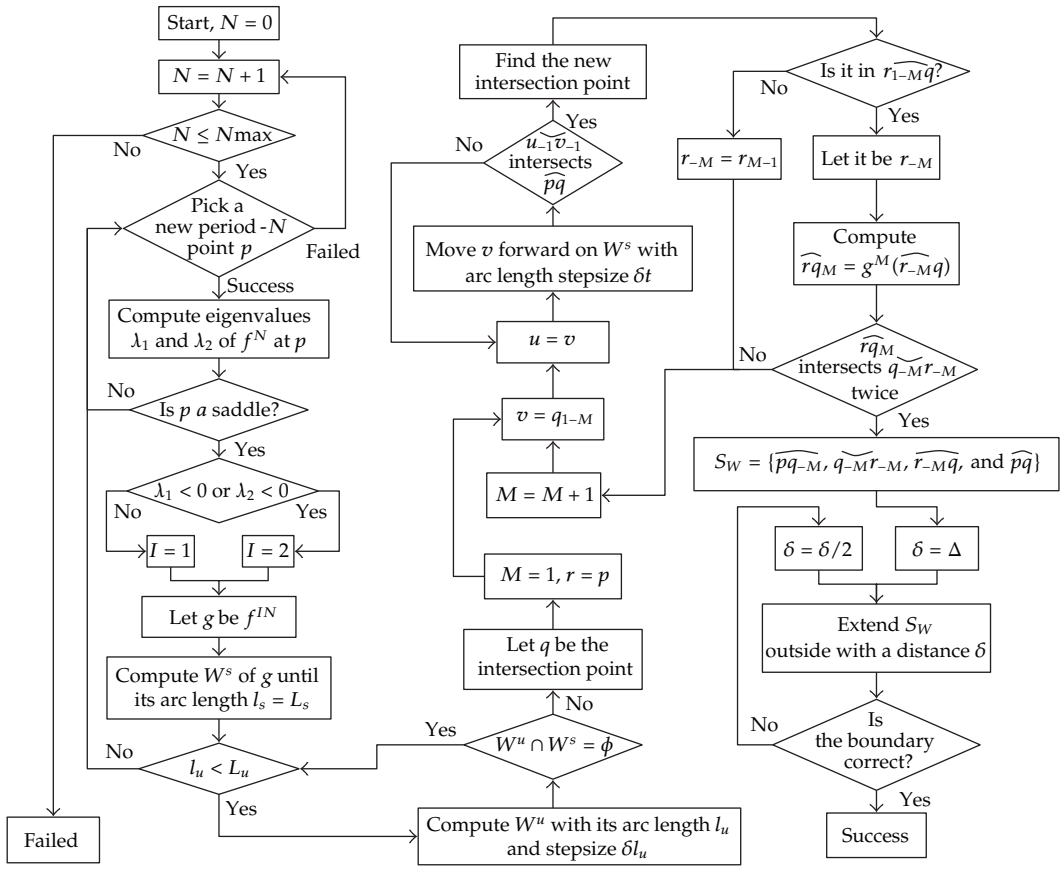

Figure 2: The flowchart of the algorithm.

the image of $\widehat{r_{-M}q}$ under the map g^M. If $\widehat{rq_M}$ does not intersect the new $\overbrace{q_{-M}r_{-M}}$ twice, we increase M with step 1 and try it again; otherwise, we take the manifold pieces $\widehat{pq_{-M}}$, $\overbrace{q_{-M}r_{-M}}$, $\widehat{r_{-M}q}$, and $\overbrace{qp}$ as the boundary of S_W.

(3) Extend the boundary of S_W outward with an equally small distance of δ to get a new boundary S. Then we compute the image of S under g^M, and check whether the condition of the Smale horseshoe is satisfied. Generally, the smaller the δ is, the easier the condition can be satisfied; therefore we should decrease δ when the condition fails.

Remark 3.1. The algorithm is based on a saddle with transversal homoclinic. Whether it is fully automatic depends on the procedure to detect this saddle via the periodic orbit and the manifolds computation in the first step. Fortunately, they are both fundamental problems in numerical study of dynamical systems, and there are many good algorithms and software packages in the literature to do this, for example, [11, 12]. So it can be handled by the detailed control flow shown in Figure 2.

Remark 3.2. The intersection of the stable manifold and the unstable manifold must be transversal (not tangential), which guarantees that the algorithm will terminate in a finite number of steps according to the general geometry described by Wiggins [13].

Now we demonstrate the ability and efficiency of this algorithm by finding horseshoes of several classical chaotic maps in the following four examples.

Example 1 (the Duffing map). The Duffing map is a discrete version of the Duffing equation [13]. It takes a point (x_n, y_n) in the plane and maps it to a new point given by

$$\begin{aligned} x_{n+1} &= y_n, \\ y_{n+1} &= -bx_n + ay_n - y_n^3, \end{aligned} \tag{3.1}$$

where the two parameters usually set to $a = 2.75$ and $b = 0.2$ to produce chaotic behavior. Numerical computation shows that the map has three fixed saddle points. Among them, the Jacobian matrix at the origin has two positive eigenvalues, $\lambda_1 \approx 0.07476$ and $\lambda_2 \approx 2.67524$. Clearly, $I = N = 1$, then we find a homoclinic point $q = (1.6057128, 0.1206999)$. After a process illustrated in Figure 3, where the solid lines (blue) indicate the stable manifold and the dot lines (red) indicate the unstable manifold, we detect S_w at $M = 3$, and finally find a horseshoe, as illustrated in Figure 4.

Example 2 (the Hénon map). The Hénon map, as a discrete model of the Lorenz system, is one of the most studied dynamical systems that exhibit chaotic behavior. It maps a point (x_n, y_n) in the plane to a new point given by

$$\begin{aligned} x_{n+1} &= y_n + 1 - ax_n^2, \\ y_{n+1} &= bx_n, \end{aligned} \tag{3.2}$$

where the two parameters canonically take $a = 1.4$ and $b = 0.3$ [14]. Our computation shows that the map has two fixed saddle points. We randomly choose one, that is, $p = (0.6313545, 0.1894063)$. The corresponding Jacobian matrix has one positive eigenvalue of $\lambda_1 \approx 0.155946$ and one negative eigenvalue of $\lambda_2 \approx -1.92374$. So $N = 1$ and $I = 2$. Then we find a homoclinic point $q = (0.584132, 0.101649)$. When $M = 1$, we find a horseshoe illustrated in Figure 5.

Example 3 (the Ikeda map). The Ikeda map is a discrete-time dynamical system simplified from a plane-wave model. The map is given by

$$\begin{aligned} x_{n+1} &= 1 + u\left(x_n \cos t_n - y_n \sin t_n\right), \\ y_{n+1} &= u\left(x_n \sin t_n + y_n \cos t_n\right), \end{aligned} \tag{3.3}$$

where $t_n = 0.4 - 6/(1 + x_n^2 + y_n^2)$ and u is a parameter [15]. The map has a strange attractor for $u = 0.9$. Our computation only finds one fixed saddle point, that is, $p = (0.5327546, 0.2468968)$. The corresponding Jacobian matrix has two negative eigenvalues,

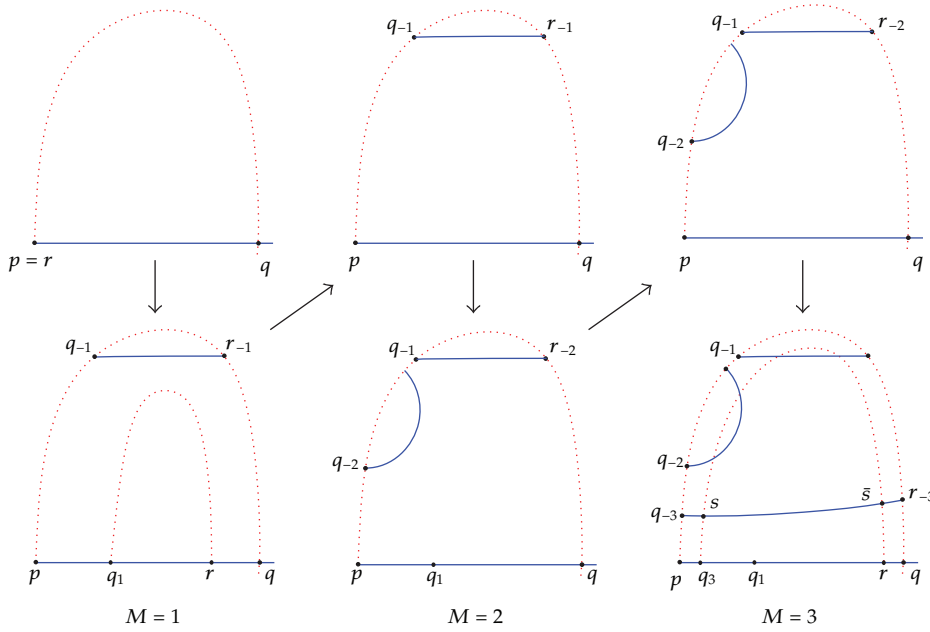

Figure 3: The process of detecting S_w.

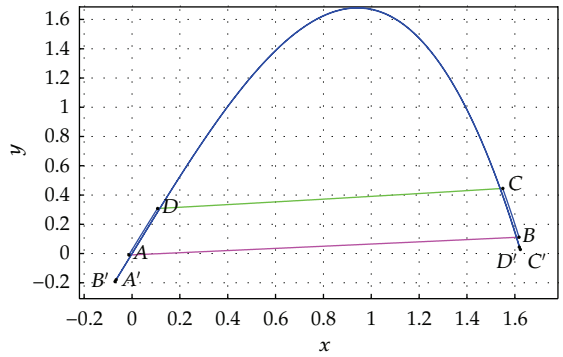

Figure 4: A Smale horseshoe found in the Duffing map.

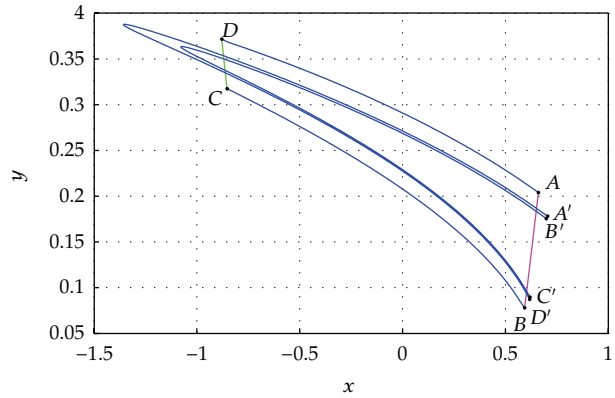

Figure 5: A Smale horseshoe found in the Hénon map.

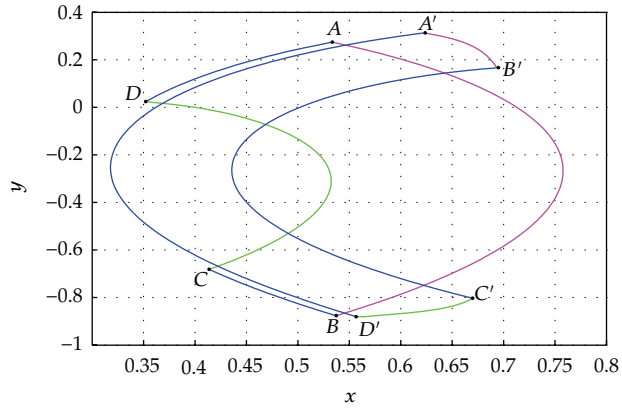

Figure 6: A Smale horseshoe found in the Ikeda map.

$\lambda_1 \approx -0.33896$ and $\lambda_2 \approx -2.38969$. Therefore, we set $N = 1$ and $I = 2$, and then find a homoclinic point $q = (0.5370113, -0.8444263)$. When $M = 1$, we find a horseshoe, illustrated in Figure 6. Because the boundary of S is automatically generated by the algorithm, it appears very different from other horseshoes in the literature where the boundaries usually are polygons.

Example 4 (the Lozi map). The Lozi map is a two-dimensional map similar to the Hénon map but with the term x_n^2 replaced by $|x_n|$. It is given by the equations

$$\begin{aligned} x_{n+1} &= 1 - a|x_n| + y_n, \\ y_{n+1} &= bx_n, \end{aligned} \tag{3.4}$$

where the two parameters also take $a = 1.4$ and $b = 0.3$. Our computation shows that the map has two fixed saddle points. However, the stable and unstable manifolds of each point do not intersect. In order to find a homoclinic point, we try period two. Consequently, we only find one period-2 obit, that is, $p = (0.8571429, -0.0857143)$, and the corresponding Jacobian matrix has two negative eigenvalues with $\lambda_1 \approx -0.06975$ and $\lambda_2 \approx -1.2902$. Obviously, $N = 2$ and $I = 2$; then, we find a homoclinic point $q = (0.849499, -0.0943964)$. When $M = 1$, we find a horseshoe, illustrated in Figure 7, finally.

Remark 3.3. The "crossing" relation between $h(S)$ and S is the key to the existence of horseshoe. The relation remains unchanged if we map $h(S)$ and S to their images by a homeomorphism. Therefore, if we find a horseshoe with a certain homoclinic point q, then we have infinitly many horseshoes just by iterating S with the system map f. On the other hand, if we find a different homoclinic point, then we may get a different horseshoe, which may be transformed from the original S under some iterations of the system map. For example, we can get a new horseshoe of the Duffing map only by changing q to $(0.1207000, 0.00902376)$. A horseshoe similar to this one, for example, that in Figure 8, can be gotten by Figure 2 under two time iterations of the Duffing map.

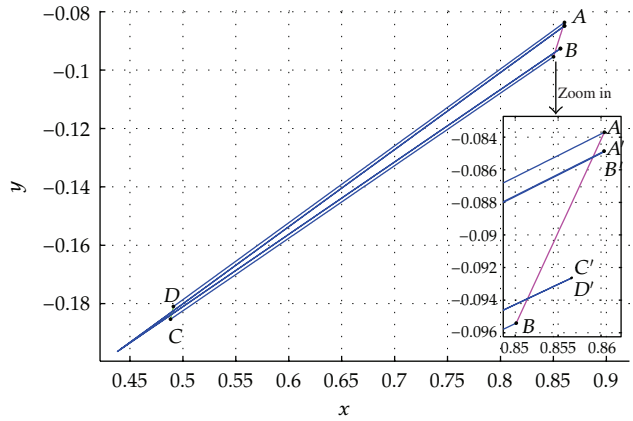

Figure 7: A Smale horseshoe found in the Lozi map.

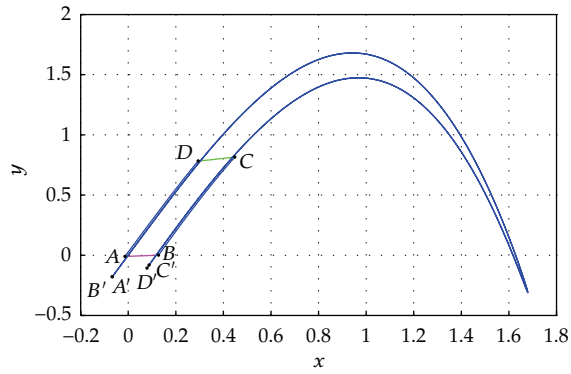

Figure 8: Another Smale horseshoe found in the Duffing map.

Table 1: The time consumed for all examples in MATLAB. (The code is downloadable from http://www.mathworks.com/matlabcentral/fileexchange/authors/27275).

Chaotic maps	Saddle detection (S)	Horseshoe detection (S)	Total (S)
The Duffing map	0.43	2.96	3.39
The Hénon map	0.27	0.73	1.00
The Ikeda map	0.48	0.92	1.40
The Lozi map	1.20	3.24	4.44

4. Conclusions

We have proposed an algorithm for finding the Smale horseshoes in 2D chaotic maps. Numerical studies for four classical maps suggest that this algorithm can effectively find their horseshoes. Comparing with [8], this method is dedicated to the Smale horseshoes in 2D maps. The advantage of the algorithm is that horseshoes can be found automatically by only a few given parameters, which is less dependent on researchers' experience. In [8], one has to find a horseshoe manually by a lot of trials, which may take hours sometime. The time consumed for the above examples is shown in Table 1, which takes a few seconds at most. So

the algorithm is more efficient. In the algorithm, each side of the boundaries is a curve taken parallel along a stable or unstable manifold. This way, the existence of a Smale horseshoe is guaranteed. From this point of view, the algorithm is more applicable than methods using rectangles or polygons to compose boundaries, for example, [8].

Acknowledgments

The authors are very grateful to the reviewers for their valuable comments and suggestions. This work was supported in part by the National Natural Science Foundation of China (61104150, 10972082), by the Natural Science Foundation Project of Chongqing (cstcjjA40044), and by the Youth Foundation of CQUPT (A2008-26).

References

[1] X.-S. Yang, "Topological horseshoes and computer assisted verification of chaotic dynamics," *International Journal of Bifurcation and Chaos*, vol. 19, no. 4, pp. 1127–1145, 2009.

[2] J. Kennedy and J. Yorke, "Topological horseshoes," *Transactions of the American Mathematical Society*, vol. 353, no. 6, pp. 2513–2530, 2001.

[3] X. S. Yang, H. Li, and Y. Huang, "A planar topological horseshoe theory with applications to computer verifications of chaos," *Journal of Physics A: Mathematical and General*, vol. 38, no. 19, pp. 4175–4185, 2005.

[4] P. Zgliczyński and M. Gidea, "Covering relations for multidimensional dynamical systems," *Journal of Differential Equations*, vol. 202, no. 1, pp. 32–58, 2004.

[5] Q. Li and X. Yang, "A 3D Smale horseshoe in a hyperchaotic discrete-time system," *Discrete Dynamics in Nature and Society*, vol. 2007, Article ID 16239, 9 pages, 2007.

[6] B. Bánhelyi, T. Csendes, and B. M. Garay, "Optimization and the miranda approach in detecting horseshoe-type Chaos by computer," *International Journal of Bifurcation and Chaos*, vol. 17, no. 3, pp. 735–747, 2007.

[7] X. Yang and Q. Li, "A computer-assisted proof of chaos in Josephson junctions," *Chaos, Solitons and Fractals*, vol. 27, no. 1, pp. 25–30, 2006.

[8] Q. Li and X.-S. Yang, "A simple method for finding topological horseshoes," *International Journal of Bifurcation and Chaos*, vol. 20, no. 2, pp. 467–478, 2010.

[9] Q. Li, S. Chen, and P. Zhou, "Horseshoe and entropy in a fractional-order unified system," *Chinese Physics B*, vol. 20, no. 1, Article ID 010502, 6 pages, 2011.

[10] Q. Li, X.-S. Yang, and S. Chen, "Hyperchaos in a spacecraft power system," *International Journal of Bifurcation and Chaos*, vol. 21, no. 6, pp. 1719–1726, 2011.

[11] B. Krauskopf and H. Osinga, "Growing 1D and quasi-2D unstable manifolds of maps," *Journal of Computational Physics*, vol. 146, no. 1, pp. 404–419, 1998.

[12] E. Doedel, A. Champneys, T. Fairgrieve et al., "AUTO 97: continuation and bifurcation software for Ordinary Differential Equations (with HomCont)".

[13] S. Wiggins, *Introduction to Applied Nonlinear Dynamical Systems and Chaos*, vol. 2, Springer, New York, NY, USA, 2nd edition, 2003.

[14] M. Hénon, "A two-dimensional mapping with a strange attractor," *Communications in Mathematical Physics*, vol. 50, no. 1, pp. 69–77, 1976.

[15] S. Hammel, C. Jones, and J. Moloney, "Global dynamical behavior of the optical field in a ring cavity," *Optical Society of America, Journal B: Optical Physics*, vol. 2, pp. 552–564, 1985.